

Study on the Effect of Chlorogenic Acid on Prosthetic Joint Infection Biofilm Based on Eno Gene Testing

Jie Lin

Ningbo Chinese Medicine Hospital, Ningbo, 315100, Zhejiang, China

Background: Chlorogenic acid, a natural polyphenol found abundantly in plants such as honeysuckle and eucommia, possesses broad-spectrum antimicrobial properties with complex mechanisms. Its efficacy in combating biofilms formed by pathogenic bacteria during prosthetic joint infection (PJI) warrants further investigation.

Purpose: This study aimed to establish an *in vitro* model of PJI, extract RNA eluate samples treated with specific concentrations of chlorogenic acid, perform eno gene detection via polymerase chain reaction (PCR), and assess chlorogenic acid's ability to disrupt biofilms formed by PJI pathogens by analyzing detection rates and efficiency.

Methods: Five common PJI pathogens were cultured at 37°C in monoclonal tryptic soy broth. Glass slides were incubated in a shaker at 37°C for 48 hours to simulate biofilm formation. Samples were divided into distilled water control and chlorogenic acid treatment groups. RNA eluates were extracted using ultrasonic disruption and subjected to eno gene PCR testing. Differences in eno gene detection rates and efficiency between the groups were analyzed.

Results: In the distilled water control group, the eno gene detection rate was 44.4% with 53.8% accuracy. In the chlorogenic acid group, the eno gene detection rate increased to 66.6% with 73.3% accuracy. Chlorogenic acid treatment significantly improved detection rates and efficiency. Compared with the control, chlorogenic acid-treated samples consistently showed robust positive results less prone to confusion or interference.

Conclusion: Biofilm formation by pathogenic bacteria closely correlates with PJI development, influencing the detection of specific eno genes. Chlorogenic acid effectively disrupts PJI pathogen biofilms, markedly enhancing eno gene detection rates and accuracy.

Posttreatment, positive results demonstrate strong and reliable outcomes less susceptible to interference.

Key words: Prosthetic joint infection – Eno gene – Chlorogenic acid – Biofilm

Prosthesis joint infection (PJI) represents the most severe complication following total joint replacement surgery.^{1,2} The occurrence of PJI correlates closely with the formation of biofilms by pathogenic bacteria. These biofilms rapidly create a protective barrier around the bacteria during PJI, shielding them from both the human immune system and antibiotics. This barrier also obstructs the detection of “live” pathogenic bacteria and their specific genes from clinical samples.^{3–6}

Chlorogenic acid (CGA) is a phenylpropanoid compound synthesized by plants through the shikimate pathway during aerobic respiration. It is widely present in medicinal herbs, such as honeysuckle, eucommia, and coffee, as well as various foods.⁷ CGA demonstrates excellent biocompatibility and safety in humans, showing no significant adverse effects. Recent research suggests that CGA can effectively inhibit and disrupt biofilms formed by pathogenic bacteria through multiple pathways. This property is considered pivotal in CGA’s potential therapeutic role in treating PJI.^{8,9} However, further exploration is needed to fully understand the specific mechanisms of CGA action and its effects on biofilms formed by different strains of pathogenic bacteria.¹⁰

The *eno* gene is a specific genetic marker closely linked to biofilm formation by *Staphylococcus*, the most prevalent and significant pathogen in PJI. Recent studies have demonstrated that the *eno* gene exhibits the highest detection rate and efficiency among genes examined for PJI pathogens.^{11,12} This study aimed to establish an *in vitro* model of PJI, extract RNA eluates, and compare *eno* gene detection results between samples treated with distilled water (control group) and samples treated with CGA. The research investigates the role of CGA in disrupting biofilms during the treatment of PJI.

Materials and Methods

Materials

Main strains and sources

The bacterial strains used in this experiment include *Staphylococcus aureus* (ATCC 25923), *Staphylococcus epidermidis* (ATCC 12228), methicillin-resistant *Staphylococcus aureus* (MRSA, ATCC 43300), and *Escherichia*

coli strains (ATCC 8739 and ATCC 25922). All strains were sourced from the Key Laboratory of Orthopedic Implant Infection at Shanghai Municipal Hospital.

Main instruments

The primary instruments used in this study included a Sigma 3-16k centrifuge (Chicago, Illinois, USA), uQuant microplate spectrophotometer (USA), MAX-IMA ultrapure water system (London, UK), Densi-check PLUS Merieux turbidimeter (USA), Densicheck PLUS constant temperature shaking incubator (Loveland, Colorado, USA), U57085 ultralow temperature freezer (UK), Bio-RAD pac3000 electrophoresis system (USA), PROFI-LINE constant temperature incubator (Berlin, Germany), OPTIGEL-12 laminar flow cabinet (France), HM-202 electronic balance (Tokyo, Japan), Christ101042 vacuum freeze dryer (Paris, France), U200S-control ultrasonic homogenizer (Munich, Germany), KS-120EI ultrasonic cleaner (manufactured by Ningbo Haishu Kesheng), trypticase soy broth (TSB) culture medium (London, UK), and trypticase soy agar (TSA) plates (London, UK).

Methods

Bacterial cultivation

Frozen stocks of *Staphylococcus aureus* (ATCC 25923), *Staphylococcus epidermidis* (ATCC 12228), methicillin-resistant *Staphylococcus aureus* (MRSA, ATCC 43300), *Escherichia coli* (ATCC 8739), and *Escherichia coli* (ATCC 25922) strains were streaked onto blood agar plates using the quadrant streak method. The plates were then statically incubated at 37°C for 24 hours. Single colonies were selected and transferred into 10-mL sterile glass tubes containing 3 mL of TSB. These tubes were placed on a shaker at 130 rpm under aerobic conditions at 37°C for 12 hours. The bacterial cultures underwent two successive passages in fresh TSB medium. After each passage, bacterial suspensions were centrifuged at 8,000g for 10 minutes. The pellets were resuspended in fresh TSB to achieve a concentration of 1.0×10^6 colony-forming units/mL, adjusted using the McFarland turbidity method.

Experimental groups

A total of 41 samples were included in the experiment, divided into 2 batches. The first batch comprised

Table 1 Experimental groups

Group name	Bacterial strain	Sample no.
Distilled water control group	ATCC25923 (<i>S. aureus</i>)	C, F ^a , H ^a , B+, C+, H+ ^a
	ATCC12228 (<i>S. epidermidis</i>)	B, D ^a , L ^a , E+, F+, J+
	ATCC43300 (MRSA)	G, I, K ^a , A+ ^a , D+, G+ ^a
	ATCC8739 (<i>Escherichia coli</i>)	A ^a , M, N ^a
	ATCC25922 (<i>Escherichia coli</i>)	J, O, P
	Blank control	E, I+
Chlorogenic acid treatment group	ATCC25923 (<i>S. aureus</i>)	1 ^a , 7 ^a , 11 ^a
	ATCC12228 (<i>S. epidermidis</i>)	5, 9 ^a , 10
	ATCC43300 (MRSA)	6 ^a , 13 ^a , 14
	ATCC8739 (<i>Escherichia coli</i>)	3, 4, 12
	ATCC25922 (<i>Escherichia coli</i>)	2, 8, 15 ^a

^aPositive sample.

26 samples treated with distilled water (distilled water control group), consisting of 24 samples with bacterial cultures and 2 sterile control samples. The second batch included 15 samples treated with CGA (CGA treatment group), all of which were bacterial culture positive. The bacterial strains used in the experiment encompassed 5 different ATCC codes, all representing common pathogens in PJI (Table 1).

Biofilm formation assay

The tissue culture plate is widely employed for quantitative cultivation and assessment of biofilms. Standard flat-bottomed, 96-well culture plates were used. Bacterial suspensions containing the specified samples were inoculated into each well with a final volume of 200 µl per well. The plates were statically incubated at 37°C for 24 hours. Following removal of the culture medium, wells were gently washed 3 times with 0.01 mol/L pH 7.4 phosphate-buffered saline buffer to remove free-floating bacteria. Subsequently, the plates were dried in a 60°C oven for 1 hour. Next, 200 µl of 0.1% crystal violet solution was added to each well and incubated at room temperature for 5 minutes for staining. Excess stain was discarded, and wells were washed 3 times with double-distilled water to remove residual dye. The plates were then dried at 37°C for 2 hours. Each well received 200 µl of 30% acetic acid solution for 10 minutes to dissolve the crystal violet. Absorbance was measured at 492 nm using a microplate reader to quantify biofilm formation with results reported as A_{492} values.

Establishment of *in vitro* PJI model

Frozen bacterial strains, including staphylococcus aureus (ATCC 25923), staphylococcus epidermidis (ATCC 12228), MRSA (ATCC 43300), escherichia

coli (ATCC 8739), and escherichia coli (ATCC 25922), were streaked onto blood agar plates using quadrant streaking. The plates were statically cultured at 37°C for 24 hours, totaling 39 plates inoculated with 5 different bacterial strains. Single colonies were selected and inoculated into 10-ml sterile glass tubes containing 3 ml of TSB for aerobic culture at 37°C for 24 hours. The tubes were then placed on a shaker at 120 rpm under aerobic conditions at 37°C for 48 hours. The bacterial suspensions underwent dynamic cultivation twice in fresh TSB medium. Following centrifugation at 8,000g for 10 minutes, the bacterial density was adjusted to 0.5 McFarland using fresh TSB medium. Standard 96-well tissue culture plates were utilized with each well containing 200 µl of bacterial suspension. After static incubation at 37°C for 24 hours, the culture medium was gently aspirated. Each well was washed 3 times with 0.01 mol/L PBS buffer (pH 7.4) to remove free-floating bacteria. The plates were then air-dried in a 60°C oven for 1 hour. Subsequently, 200 µl of 0.1% crystal violet solution was added to each well and allowed to stain for 5 minutes at room temperature. After discarding the staining solution, the wells were rinsed 3 times with distilled water to remove excess stain. The plates were dried at 37°C for 2 hours. Next, 200 µl of 30% acetic acid solution was added to each well and allowed to dissolve the dye for 10 minutes. The absorbance at 492 nm was measured using a microplate reader to obtain the A_{492} value, representing the biofilm formation. For the distilled water control group, 5 ml of distilled water was added and allowed to stand for 4 hours. For the CGA treatment group, 5 ml of CGA at a concentration of 128 µg/ml was added and allowed to stand for 4 hours, prepared for subsequent RT-PCR testing.

Table 2 Diagnostic efficiency determination

	Actual gene PCR testing results	Expected results as per experimental design
True positive (A)	Positive (+)	Positive (+)
False positive (B)	Positive (+)	Negative (–)
True negative (C)	Negative (–)	Negative (–)
False negative (D)	Negative (–)	Positive (+)

Fluorescence quantitative PCR experiment

The primer sequences for the *eno* gene were synthesized by Shanghai Sangon Biotech. PCR targeted amplification of the gene of interest using reverse-transcribed products from the same reaction system. Prior to conducting fluorescence quantitative PCR (qPCR), DNA extraction and purification were performed. Subsequently, gel electrophoresis was used for imaging with gel images scanned and stored using a gel imaging system.

Statistical analysis of data

RT-PCR images were analyzed from 3 repeated experiments. Gel electrophoresis images were scanned and analyzed for grayscale intensity using the Bio-Rad ChemiDoc MP gel imaging system. Each sample was tested in triplicate, and experimental results were reported in terms of detection rate, sensitivity, specificity, and accuracy for different genes. Based on experimental design and literature, the diagnostic efficiency of each gene was calculated by comparing PCR results with the intended test outcomes (diagnostic efficiency criteria are detailed in Table 2).

Based on Table 2, the diagnostic outcomes are classified into 4 categories: true positive (A), false positive (B), true negative (C), and false negative (D), denoted as A, B, C, and D, respectively. The detection rate is calculated as $A/(A+D)$, which reflects the test's capability to identify positive results. Specificity, or true negative rate, is determined by $C/(B+C)$, indicating the test's ability to correctly exclude positive results. Higher specificity correlates with lower potential for misdiagnosis. Accuracy of the test, defined as $(A+C)/(A+B+C+D)$, offers a comprehensive assessment of diagnostic performance.

Results

Biofilm production capability assessment of experimental bacterial strains

Using the tissue culture plate method, biofilm growth was quantified by measuring changes in absorbance values with crystal violet. An A₄₉₂ value above 0.3

indicates sufficient biofilm formation by pathogenic strains in the culture system, confirming the successful establishment of the *in vitro* PJI model. The assessment revealed average OD₄₉₂ values of 0.493 (*Staphylococcus aureus* ATCC 25923), 0.489 (*Staphylococcus epidermidis* ATCC 12228), 0.476 (MRSA ATCC 43300), 0.488 (*Escherichia coli* ATCC 8739), and 0.478 (*Escherichia coli* ATCC 25922) in TSB samples. These findings demonstrate that all tested strains were capable of forming biofilms in this culture system, validating the successful establishment of the *in vitro* PJI model.

PCR testing results of *eno* gene in the distilled water group

The PCR results for *eno* gene in the distilled water group showed that samples A, D, F, H, K, L, N, A+, G+, and H+ tested positive, whereas the rest tested negative (Fig. 1). According to Table 2, which assesses diagnostic efficiency, the distilled water group had 8 true positives and 10 false negatives in *eno* gene detection, yielding a detection rate of 44.4%. Moreover, there were 6 true negatives and 2 false positives, resulting in a specificity of 75%. The calculated accuracy of *eno* gene PCR testing in the distilled water group was 53.8%.

PCR testing results of *eno* gene in the CGA treatment group

The PCR results for the *eno* gene in the CGA treatment group indicated that samples 1, 6, 7, 9, 11, 13, and 15 tested positive, whereas the remaining samples tested negative (Fig. 2). Compared with the varied intensities of positive results in the distilled water control group, all positive results in the CGA treatment group exhibited strong positivity. This strong positivity ensures that these results are less susceptible to oversight, confusion, or interference during actual testing. According to Table 2, which assesses diagnostic efficiency, the CGA treatment group had 6 true positives and 3 false negatives in *eno* gene detection, resulting in a detection rate of 66.6%. Moreover, there were 5 true negatives and 1 false positive, establishing a specificity of 83%. The calculated accuracy of *eno* gene PCR testing in the CGA treatment group was 73.3%.

Discussion

Biofilm formation plays a critical role in the pathogenesis of PJI.^{3–5} Pathogenic biofilms act as natural barriers, enhancing resistance against antimicrobial

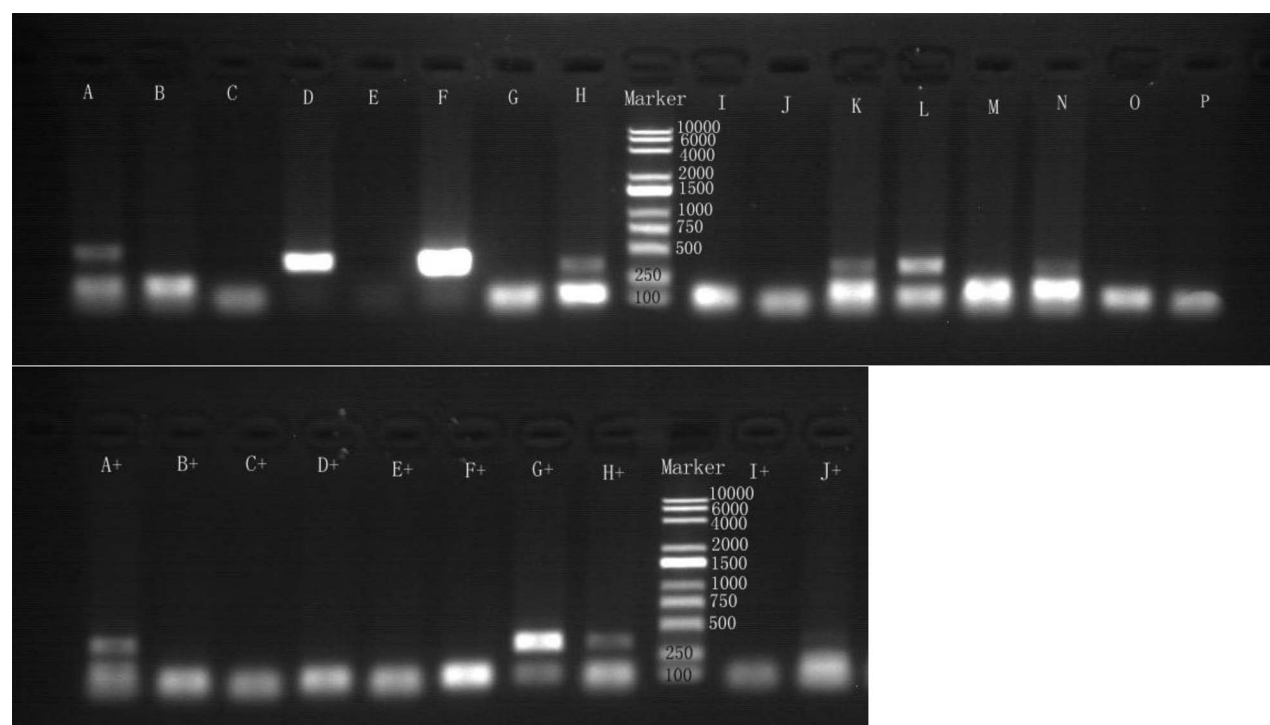


Fig. 1 PCR testing results of eno gene in the distilled water group.

agents and host immune responses, posing a significant challenge in clinical management.¹³

Traditional Chinese medicine, renowned for its diverse origins, minimal adverse effects, precise therapeutic efficacy, and reduced likelihood of inducing bacterial resistance, has garnered increasing attention for its potential in combating biofilm-related infections.^{14,15} CGA, a phenolic compound synthesized via the shikimate pathway during aerobic respiration in plants, is naturally present in several traditional Chinese medicinal herbs and dietary sources such as honeysuckle, eucommia bark, and coffee. It demonstrates notable inhibitory effects against common pathogens

associated with PJI, including various *Staphylococcus* species.^{16,17} Recent studies have underscored CGA's antimicrobial action primarily through pathways that inhibit and disrupt pathogenic biofilms.^{18,19}

The eno gene, encompassing genes crucial for biofilm formation in *Staphylococcus aureus*, *Staphylococcus epidermidis*, and MRSA, encodes adhesive proteins pivotal for staphylococcal surface attachment.²⁰ Recent research highlights the eno gene's superior efficiency in detecting genes relevant to PJI pathogens,^{11,12,21} justifying its selection in experimental protocols. The protective role of biofilms shields pathogens, potentially masking the detection

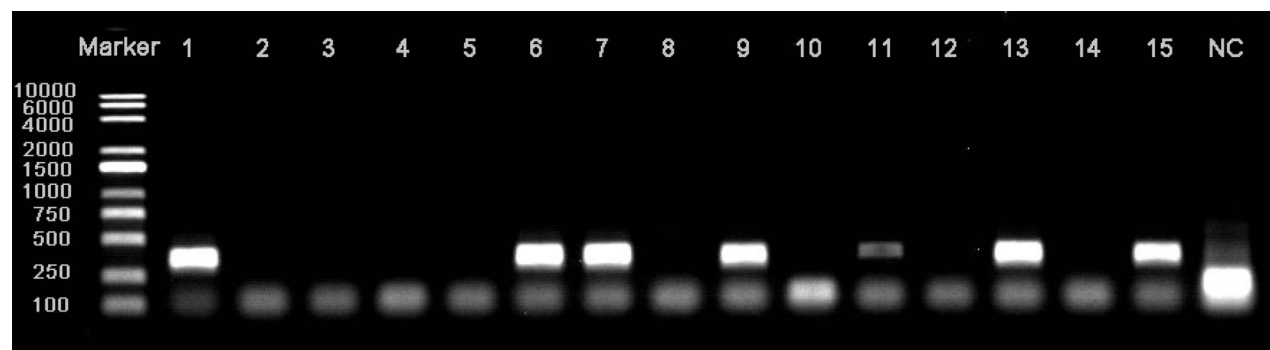


Fig. 2 PCR testing results of eno gene in the chlorogenic acid group.

of specific genes in experimental samples. Comparative analysis of eno gene detection rates across experimental samples provides initial insights into CGA's potential to disrupt pathogenic biofilms.

Discussion on eno gene PCR testing results of the distilled water control group

In the experimental samples of the distilled water control group, one false positive result was detected among the 6 *Escherichia coli* samples. Additionally, within the 18 samples from the 3 *Staphylococcus* groups, there were 10 instances of false negative results, whereas the 2 sterile blank samples both tested negative. Based on these findings, the detection rate of the eno gene in the distilled water control group was calculated at 44.4% with a specificity of 75% and an accuracy of 53.8%.

The eno gene is specific to *Staphylococcus* species, and therefore, samples from the *Escherichia coli* group and sterile blank control group should ideally yield negative results. Indeed, the actual testing confirmed this expectation except for 1 false positive result in the *Escherichia coli* ATCC 8739 group, in which the remaining samples from both groups tested negative.

As a specific marker for *Staphylococcus*, the eno gene is found in *Staphylococcus aureus*, *Staphylococcus epidermidis*, and MRSA strains. Consequently, all 3 *Staphylococcus* groups should theoretically test positive for the gene. However, the observed 10 false negative results among the 18 samples from the *Staphylococcus aureus*, *Staphylococcus epidermidis*, and MRSA groups indicate a lower than expected detection rate for the eno gene alongside varied intensity in positive detection outcomes. Possible reasons for these negative results include false negatives, potentially caused by primer design issues or biofilm presence hindering the detection of the eno gene. Alternatively, true negatives may suggest that the eno gene might not serve effectively as a diagnostic marker in detecting *Staphylococcus* infections within the tested samples.

Discussion on eno gene PCR testing results of the CGA treatment group

In the experimental samples of the CGA treatment group, 1 false positive result was detected among the 6 *Escherichia coli* samples. Additionally, among the 9 samples from the 3 *Staphylococcus* groups, there were 3 instances of false negative results with the negative control yielding normal results. Based on these findings, the eno gene detection rate in the

CGA treatment group was calculated to be 75% with a specificity of 83% and an accuracy of 73.3%.

The eno gene in the CGA treatment group not only demonstrated a high detection rate but also exhibited good specificity in detection. Compared with the distilled water control group, the results showed strong positives that were less susceptible to interference or confusion. Based on the eno gene testing outcomes from the CGA treatment group, we confidently exclude the possibility of true negatives in the distilled water group and mitigate the potential for false negatives due to primer design issues.

Comparison of eno gene testing outcomes between the CGA treatment group and the distilled water control group clearly indicates a significant enhancement in the detection rate and efficiency of the eno gene in *Staphylococcus*-related PJI. However, it is important to acknowledge that these results may be influenced by various other factors. Furthermore, the prevalence of strong positives observed in the eno-positive results of the CGA group confirms that CGA not only improves gene detection efficiency by inhibiting and disrupting pathogenic biofilms but also enhances detection outcomes with strong positives.

Conclusion

This study demonstrates that CGA enhances the detection rate and efficiency of the eno gene by disrupting pathogenic biofilms, resulting in consistently strong positive detection outcomes. In practical clinical applications, employing CGA to disrupt pathogenic biofilms, combined with antibiotic therapy, can greatly enhance the treatment efficacy of PJI.

Limitations

The role of CGA in the treatment of PJI is multifaceted. They not only effectively inhibit and disrupt pathogenic biofilms but also exert therapeutic effects by activating the human immune system and modulating inflammatory responses. This study, conducted *in vitro*, specifically investigates the inhibitory effects of CGA on pathogenic biofilms without exploring the direct response of the human body to CGA itself. Moreover, the experimental strains are derived from standard bacterial cultures, potentially differing from clinical strains detected in actual PJI infections due to the complex nature of clinical scenarios.

Acknowledgments

The author declare that they have no conflict of interest. The data that support this study are available

from the corresponding authors upon request. This study was supported by the Zhejiang Traditional Chinese Medicine Administration (Grant No. 2023ZF160). All the authors have read and approved the final manuscript. The following are the author contributions: Jie Lin contributed to research design and acquisition, drafted the manuscript and revised it critically; all authors read and approved the final manuscript.

© 2025 Lin; licensee The International College of Surgeons. This is an Open Access article distributed under the terms of the Creative Commons Attribution Noncommercial License which permits use, distribution, and reproduction in any medium, provided the original work is properly cited, the use is noncommercial and is otherwise in compliance with the license. See: <http://creativecommons.org/licenses/by-nc/3.0>

References

- Kucukdurmaz F, Parvizi J. The prevention of periprosthetic joint infections. *Open Orthop J* 2016;**10**:589–599
- Goswami K, Parvizi J, Courtney PM. Current recommendations for the diagnosis of acute and chronic PJI for hip and knee—cell counts, alpha-defensin, leukocyte esterase, next-generation sequencing. *Curr Rev Musculoskelet Med* 2018;**11**(3):428–438
- Davidson DJ, Spratt D, Liddle AD. Implant materials and prosthetic joint infection: the battle with the biofilm. *EFORT Open Rev* 2019;**4**(11):633–639
- Palan J, Nolan C, Sarantos K, Westerman R, King R, Foguet P. Culture-negative periprosthetic joint infections. *EFORT Open Rev* 2019;**4**(10):585–594
- Yin W, Wang Y, Liu L, He J. Biofilms: the microbial “protective clothing” in extreme environments. *Int J Mol Sci* 2019;**20**(14):3423
- Schilcher K, Horswill AR. Staphylococcal biofilm development: structure, regulation, and treatment strategies. *Microbiol Mol Bio Rev* 2020;**84**(3):e00026-19
- Bagdas D, Gul Z, Meade J, Cam B, Clinkilic N, Gurun MS. Pharmacologic overview of chlorogenic acid and its metabolites in chronic pain and inflammation. *Curr Neuroparmacol* 2020;**18**(3):216–228
- Jiawei Y. Study on the antibacterial effect of the components of traditional Chinese medicine on clinically isolated staphylococcus aureus from periprosthetic joint infection. Guangzhou: Guangzhou University of Chinese Medicine, 2021
- Haitao Z, Pengfei X, Wenjun F, Houran C, Jinlun C, Peng D, et al. Action mechanism of Wuwei Xiaodu Yin in the treatment of periprosthetic joint infection based on network pharmacology. *Chinese J Tissue Eng Res* 2020;**24**(36):5843–5849
- Naveed M, Hejazi V, Abbas M, Kamboh AA, Khan GJ, Shumzaid M, et al. Chlorogenic acid (CGA): a pharmacological review and call for further research. *Biomed Pharmacother* 2018;**97**:67–74
- Lin J, Jin Y, Pang QJ. Application of eno and sarA gene testing in early diagnosis of periprosthetic joint infection. *Anat Res* 2021;**43**(6):609–613
- Lin J. Experimental study of gene sequential testing applied in early diagnosis of prosthetic joint infection. Ningbo: Ningbo University, 2020
- Xin Y, Chirume WM, Yixiang L, Yue F. Research progress of new treatment options for clinical bacterial biofilm infection. *West China Med J* 2023;**38**(8):1276–1280
- Tonghui W, Baodong L. Research progress of traditional Chinese medicine against bacterial biofilm. *Pharmacol Clinics Chinese Mater Med* 2021;**37**(1):260–264
- Mei H, Yuqing T, Jun L, Liu L, Wang Y. Antimicrobial resistance of Chinese herbal medicine. *Chinese J Experimental Traditional Med Formulae* 2018;**2**(23):218–224
- Yangyu L, Qingrong L, Xiaohong C, Yin W. Advances in research on the antibacterial effects and mechanism of chlorogenic acid. *Chinese J Antibiotics* 2024;**49**(2):141–150
- Chen K, Peng C, Chi F, Wang TL, Chen T. Antibacterial and antibiofilm activities of chlorogenic acid against *Yersinia enterocolitica*. *Front Microbi* 2022;**13**:885092
- Wang LB, Zhang Y, Liu Y, Wu AW. Effects of chlorogenic acid on antimicrobial, antivirulence, and anti-quorum sensing of carbapenem-resistant *Klebsiella pneumoniae*. *Front Microbi* 2022;**13**:997310
- Rajasekharan SK, Ramesh S, Satish AS, Lee J. Antibiofilm and anti-beta-Lactamase activities of burdock root extract and chlorogenic acid against *Klebsiella pneumoniae*. *J Microbiol Biotechnol* 2017;**27**(3):542–551
- Kivanc SA, Arik G, Akova-Budak B, Kvan M. Biofilm forming capacity and antibiotic susceptibility of *Staphylococcus* spp. with the icaA/icaD/bap genotype isolated from ocular surface of patients with diabetes. *Malawi Med J* 2018;**30**(4):243–249
- Lin J, Chen H, Jin Y. Research progress of the value of pathogenic bacteria in early diagnosis of periprosthetic joint infection. *Anat Res* 2023;**45**(5):470–474